BBA - Biomembranes 1862 (2020) 183193

Contents lists available at ScienceDirect

BBA - Biomembranes

journal homepage: www.elsevier.com/locate/bbamem

Review

# Isolation of intramembrane proteases in membrane-like environments

Marta Barniol-Xicota[a], Steven H.L. Verhelst[a,b,*]

[a] KU Leuven, Department of Cellular and Molecular Medicine, Laboratory of Chemical Biology, Herestraat 49, Box 802, B-3000, Belgium
[b] Leibniz Institute for Analytical Sciences, ISAS, e.V., Otto-Hahn-Str. 6b, 44227 Dortmund, Germany

ARTICLE INFO

*Keywords:*
Intramembrane proteases
Solubilization
Detergents
Liposomes
Amphipols
Lipid protein nanodiscs

ABSTRACT

Intramembrane proteases (IMPs) are proteolytic enzymes embedded in the lipid bilayer, where they cleave transmembrane substrates. The importance of IMPs relies on their role in a wide variety of cellular processes and diseases. In order to study the activity and function of IMPs, their purified form is often desired. The production of pure and active IMPs has proven to be a challenging task. This process unavoidably requires the use of solubilizing agents that will, to some extent, alter the native environment of these proteases. In this review we present the current solubilization and reconstitution techniques that have been applied to IMPs. In addition, we describe how these techniques had an influence on the activity and structural studies of IMPs, focusing on rhomboid proteases and γ-secretase.

## 1. Introduction

The discovery of site-2 protease (S2P) as a first intramembrane protease (IMP) in 1997 marked the beginning of the field of intramembrane proteolysis [1]. Since this first discovery, four different catalytic types of IMPs have been identified (Table 2): (1) *Metallo IMPs*, such as S2P. (2) *Serine IMPs*, also known as rhomboid proteases. (3) *Glutamyl IMPs*, the only member of which is Rce1. (4) *Aspartic IMPs*, exemplified by signal peptide peptidase (SPP) and the presenilin (PS) subunit of the γ-secretase complex. Some bacterial aspartic IMPs are also called presenilin homologs (PSHs). Note that the γ-secretase complex contains three additional proteins: presenilin enhancer 2 (PEN2), nicastrin (Nct) and anterior pharynx defective 1 (Aph-1). Extensive research in the last two decades has made clear that IMPs play various roles in cellular physiology [2], including ER-associated degradation [3], transcription factor release in mammalian [4] and bacterial [5] cells, and maturation of prenylated proteins [6]. IMPs also represent potential drug targets [7] as they have been linked to the pathology of several human diseases, such as Alzheimer's disease [8] and infection by apicomplexan parasites [9].

Biological membranes form the barriers between different organelles and the cytosol or the cytosol and the extracellular environment. Proteins that are embedded in these membranes, such as ion channels, g-protein coupled receptors and IMPs, allow the different compartments to communicate with each other. The hydrophobic nature of the lipid bilayer requires IMPs to have a different structure than their soluble counterparts. IMPs are composed of multiple transmembrane helices (TMHs) connected to each other with small or large loops (Fig. 1A–B). Occasionally, they also carry cytosolic or extracellular domains.

The isolation or purification of IMPs from their cellular environment serves multiple purposes. First of all, cleavage of a substrate by a purified IMP provides direct biochemical evidence for the catalysis of proteolysis. This can be especially useful when cleavage products cannot be observed because they are further degraded by other proteases in the cell. For example, cleavage of RseA by RseP (the *E. coli* homolog of S2P) is immediately followed by degradation mediated by the ClpXP complex. Akiyama and co-workers were able to unequivocally prove intramembrane proteolytic activity by combining purified RseA and RseP [10]. The ability to purify IMPs is perhaps even more important for application in kinetic studies, structure elucidation and inhibitor development.

As the membrane-embedded part of IMPs is generally not soluble in water, purification of IMPs from other membrane proteins needs to be preceded by a solubilization step. However, solubilization and purification may lead to inactivation of the IMP. The loss of proteolytic activity can have various underlying causes, including the elimination of lipids that are relevant for activity or structural integrity, or the dissociation of subunits (in case of the multimeric complexes). For example, gel filtration of purified *E. coli* rhomboid GlpG leads to lower enzymatic activity, probably by depletion of lipids [11]. Wolfe and co-workers found that dodecyl maltoside (DDM) solubilization of γ-secretase led to dissociation of the various subunits, resulting in several different, inactive complexes [12]. Hence, it is obvious that

* Corresponding author.
*E-mail addresses:* marta.barniolxicota@kuleuven.be (M. Barniol-Xicota), steven.verhelst@kuleuven.be (S.H.L. Verhelst).

https://doi.org/10.1016/j.bbamem.2020.183193
Received 20 September 2019; Received in revised form 7 January 2020; Accepted 10 January 2020
Available online 13 January 2020
0005-2736/ 

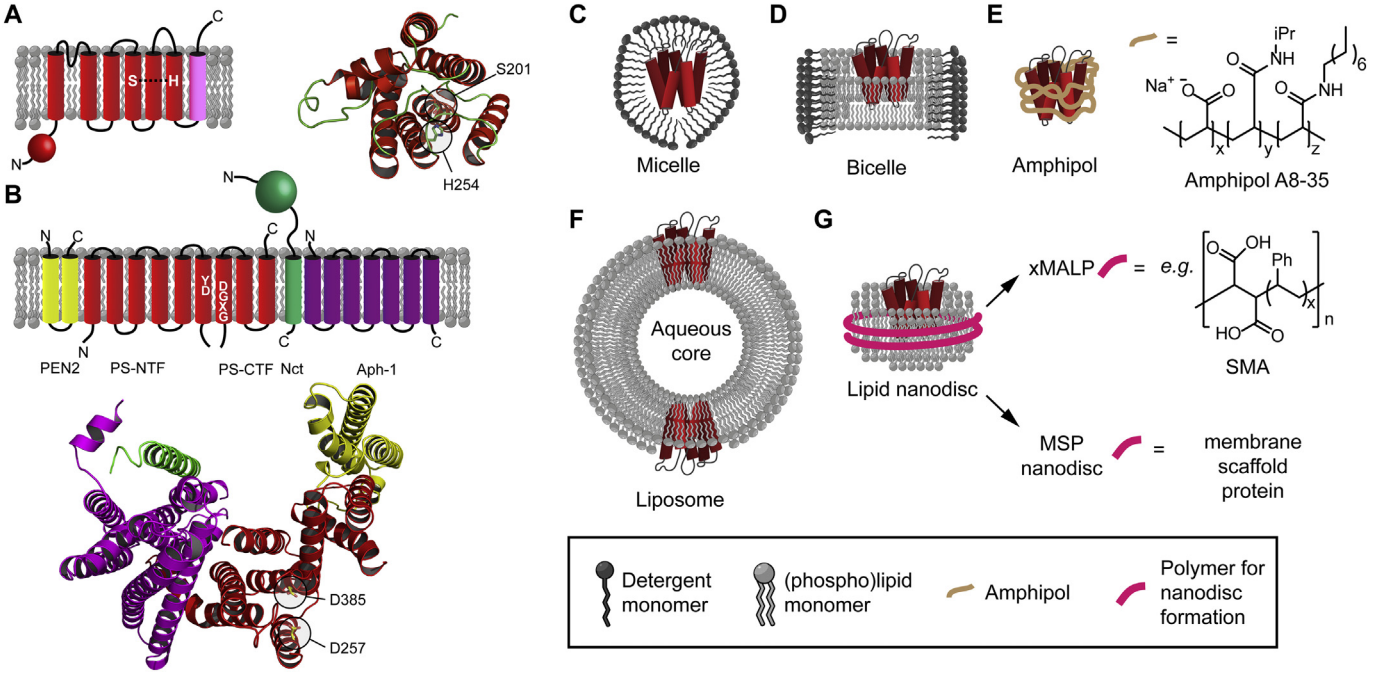


**Fig. 1.** The various membrane mimetics for IMPs. (A) Rhomboid proteases use a serine and histidine as active site residues. Their core structure consists of 6 TMHs (in red) with an optional extra TMH (in pink) at the C-terminus (as depicted here) or the N-terminus. An optional cytosolic domain may also exist. Left panel shows a schematic topology, whereas the right panel shows a top view of *E. coli* GlpG with helices in red, random coil in green and active site residues in stick representation (PDB code: 2IC8; pictures of all structures were generated with PyMol [90]). (B) The γ-secretase complex consists of four subunits: PEN2 (yellow), PS (red; split into an N-terminal and C-terminal fragment), Nct (green) and Aph-1 (magenta). Top panel shows a schematic topology and the bottom panels shows a top view of *H. sapiens* γ-secretase (PDB code: 5A63). (C) Schematic picture of a detergent-solubilized IMP in a micelle. (D) Schematic representation of an IMP in a bicelle. (E) Schematic view of an amphipol-stabilized IMP (left) and the structure of the most widely used amphipol, A8-35 (right). (F) Schematic drawing of a liposome with embedded IMPs. (G) Schematic picture of a lipid nanodisc with an embedded IMP. The polymer for nanodisc stabilization may either be a maleic acid derived polymer, such as SMA (upper panel), resulting in an xMA lipid particle (xMALP), or MSP (lower panel). For (C) and (D): note that the detergent monomers in front of the protease or the lipid bilayer are not depicted for clarity. For (F) note that only a small part of the liposome is depicted in order to show the aqueous core.

solubilization and purification procedures should be carefully chosen.

In this review article, we will summarize the current knowledge about solubilization and reconstitution of IMPs and indicate where IMP research may still benefit from methodologies that have not, or only scarcely, been applied so far. In Section 2, we will discuss the use of detergent micelles, bicelles, amphipols, liposomes and nanodiscs. An overview of acronyms of the different solubilizing agents with full names and categories is given in Table 1. In Section 3 we will highlight inhibitor development, structural elucidation and various functional studies as application areas of purified IMPs.

## 2. Solubilization methods

In order to purify an IMP – or any other membrane protein – it needs to be able to stay soluble in an aqueous environment. For this purpose its natural surrounding of the lipid bilayer of a biomembrane, with its complex composition of lipids and other membrane proteins, is usually replaced by agents that provide water solubility. Importantly, the new environment needs to provide sufficient stabilization of the protein structure.

In this section, we will discuss five different systems that mimic the membrane: (1) micelles, (2) bicelles, (3) liposomes, (4) amphipols, and (5) lipid nanodiscs (Fig. 1C–G), which all have been applied to IMPs

**Table 1**
Overview of solubilizing agents used for IMPs.

| Acronym | Full name | Category |
|---|---|---|
| A8-35 | Amphipol A8-35 | Amphipol |
| Brij-35 | Polyoxyethyleneglycol lauryl ether | Detergent (non-ionic) |
| CHAPS | 3-[(3-Cholamidopropyl)dimethylammonio]-1-propanesulfonate | Detergent (zwitterionic) |
| CHAPSO | 3-[(3-Cholamidopropyl)dimethylammonio]-2-hydroxy-1-propanesulfonate | Detergent (zwitterionic) |
| DDM | n-Dodecyl-β-D-maltoside | Detergent (non-ionic) |
| DHPC | 1,2-Dihexanoyl-sn-glycero-3-phosphocholine | Phospholipid acting as detergent (zwitterionic) |
| DIBMA | Diisobutylene maleic acid copolymer | Nanodisc forming amphipathic polymer |
| DMPC | 1,2-Dimyristoyl-sn-glycero-3-phosphocholine | Phospholipid |
| NG | n-Nonyl-β-D-glucoside | Detergent (non-ionic) |
| LMPC | 1-Myristoyl-2-hydroxy-sn-glycero-3-phosphocholine | Phospholipid acting as detergent (zwitterionic) |
| LPPG | 1-Palmitoyl-2-hydroxy-sn-glycero-3-[phospho-rac-(1-glycerol)] | Phospholipid acting as detergent (ionic) |
| SDS | Sodium dodecyl sulfate | Detergent (ionic) |
| SMA | Styrene maleic acid copolymer | Nanodisc forming amphipathic polymer |
| Triton X-100 | Polyethylene glycol *tert*-octylphenyl ether | Detergent (non-ionic) |
| UDM | Undecyl-β-D-maltoside | Detergent (non-ionic) |

**Table 2**
Overview of dates of discovery of the different catalytic types of IMPs and their solubilization/purification methods.

| Event or solubilization method | Metallo IMPs | Aspartic IMPs | | Serine IMPs | Glutamyl IMPs |
|---|---|---|---|---|---|
| | S2P | γ-Secretase[a] | SPP | Rhomboid | Rce1 |
| Discovery | 1997 [1] | 2000 [13–15] | 2002 [16] | 2001 [17,18] | 2013[b] [19] |
| Micelle[c] | 2004 [10][d] | 2002 [20][e] | 2006 [21][d] | 2005 [22,23][d,f] | 2013 [19][d] |
| Bicelle | – | – | 2015 [24][d] | 2009 [25][d] | – |
| Liposome | – | 2008 [26][g] | – | 2013 [27][f] | – |
| Amphipol | – | 2014 [28][h] | – | – | – |
| Lipid nanodisc | – | – | – | 2017 [29][d] | – |

[a] Note that γ-secretase and signal peptide peptidase (SPP) belong to the same catalytic type of aspartyl IMPs. We have given these separate columns, because of the special composition of γ-secretase, which is formed by four proteins: PS, Aph-1, PEN-2 and Nct. Note that PS and Aph-1 have two different forms, hence four different γ-secretase complexes may exist. Also note that PS is endoproteolytically cleaved into two subunits: an N-terminal fragment (PS-NTF) and a C-terminal fragment (PS-CTF).
[b] Note that Rce1 was known before as a protease, but only in 2013 it was revealed that the active site is indeed localized inside the plane of a membrane, hence classifying it as an IMP.
[c] The indicated years are those in which the respective class of IMPs was solubilized *and* purified in this system.
[d] His-tag mediated purification.
[e] Note that in this work, γ-secretase was purified by using a transition state analog, but that the identity of all subunits of the complex was still unclear.
[f] GST-tag mediated purification.
[g] Multistep immunoaffinity purification.
[h] Purification by anti-Flag affinity resin followed by gel filtration fractionation.

(Table 2). As most of these methods have been applied to rhomboids and the γ-secretase complex, we will focus our discussion on these two families of IMPs.

### 2.1. Detergent micelles

Detergents are amphipathic molecules consisting of a hydrophilic headgroup and a hydrophobic tail. There is a wide variety of detergents with different properties. They may be ionic, such as sodium dodecyl sulfate (SDS; Fig. 2A), zwitterionic, such as 3-[(3-cholamidopropyl)dimethylammonio]-2-hydroxy-1-propanesulfonate (CHAPSO, a cholic acid-derived detergent; Fig. 2B) or neutral, such as dodecyl maltoside (DDM; Fig. 2C). When added to cells or membranes pelleted by ultracentrifugation, detergents disrupt the membrane and solubilize the lipid bilayer and its embedded proteins in micelles (Fig. 1C). An important feature of a detergent is its critical micelle concentration (cmc). The cmc is the concentration of the detergent above which micelles start to form. Hence, in order to keep membrane proteins soluble, the detergent concentration needs to exceed the cmc.

All four IMP families have been solubilized and purified using detergent micelles. In 2002, Wolfe and co-workers reported the first purification of γ-secretase [20]. Although at the time, the exact composition of the complex was still elusive, previous studies on crude solubilized membranes already showed that the γ-secretase activity could be solubilized with CHAPSO [30]. Wolfe and co-workers incubated CHAPSO-solubilized membranes displaying γ-secretase activity with a hydroxyethyl urea transition state inhibitor, immobilized on an agarose matrix [20]. Elution of bound γ-secretase complex could be achieved with 1% brij-35, a non-ionic polyoxyethylene detergent. Because this detergent was not compatible with the cleavage assay using a FLAG-tagged Notch-based substrate, they used co-immunoprecipitation and a detergent exchange from brij-35 back to CHAPSO to obtain active

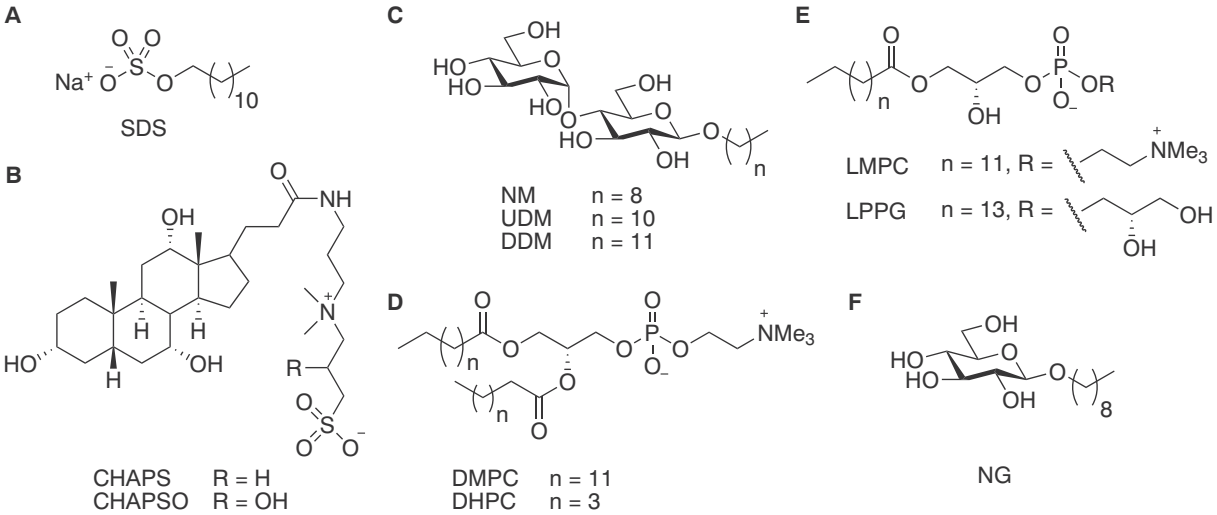


**Fig. 2.** Structures of selected detergents. (A) Ionic detergent sodium dodecyl sulfate (SDS). (B) Cholic acid derived zwitterionic detergents: 3-[(3-Cholamidopropyl) dimethylammonio]-1-propanesulfonate (CHAPS) and 3-[(3-cholamidopropyl)dimethylammonio]-2-hydroxy-1-propanesulfonate (CHAPSO). (C) Maltoside based non-ionic detergents: n-nonyl-β-D-maltoside (NM), n-undecyl-β-D-maltoside (UDM) and n-dodecyl-β-D-maltoside (DDM). (D) Phosphatidylcholine derivatives which are frequently used in combination to form bicelles: 1,2-dihexanoyl-sn-glycero-3-phosphocholine (DHPC) and 1,2-dimyristoyl-sn-glycero-3-phosphocholine (DMPC). (E) Lyso-phospholipids that form detergent micelles: 1-myristoyl-2-hydroxy-sn-glycero-3-phosphocholine (LMPC or 14:0 lyso PC) and 1-palmitoyl-2-hydroxy-sn-glycero-3-[phospho-rac-(1-glycerol)] (LPPG or 16:0 lyso PG). (F) Mild, non-ionic detergent n-nonyl-β-D-glucoside (NG).

γ-secretase, albeit captured on an IP-resin [20]. After other studies had revealed all subunits of γ-secretase [31,32], Fraering et al. used membranes of CHO cells that stably co-express all four components of the γ-secretase complex and subjected it to a multistep purification protocol, including the use of the abovementioned inhibitor-bound affinity resin and immunoaffinity purification for the GST-tagged nicastrin and/or the FLAG-tagged Pen-2 subunit [33]. With the purified protease in hand, the authors were now able to determine the effect of various additives on the activity; for example, phosphatidyl choline and sphingomyelin greatly improved γ-secretase activity [33].

Overall, γ-secretase seems sensitive to the nature of the detergent. Some detergents completely abolish activity, such as triton X-100, as it disrupts the two fragments of PS [30], or DDM, as it leads to dissociation of various subunits in a concentration dependent manner [12]. In contrast, SPP displays activity in DDM micelles [21], suggesting that the loss of activity of γ-secretase arises from the dissociation of subunits rather than being linked to DDM. Although it is unsurprising that the activity of presenilin, which depends on other membrane proteins within the γ-secretase complex, is sensitive to the nature of the detergent for solubilization, it could not be predicted that CHAPSO is the most optimal detergent for this multimeric protease complex. Apparently, CHAPSO preserves the multimeric state of γ-secretase, while it disrupts the structure of monomeric IMPs such as rhomboids [23].

Akiyama et al. described in 2004 the isolation of RseP, the *E. coli* homolog of S2P, by using DDM solubilization and his-tag mediated purification. Although the protease displayed low activity, it was capable of degrading the general protease substrate casein as well as a recombinant form of its natural substrate RseA. Importantly, the addition of 1,10-phenanthroline, a metal chelator and general metalloprotease inhibitor, or the use of active site mutant H22F completely abolished substrate cleavage, which presented evidence for the catalytic activity and the enzymatic mechanism [10]. The first purifications of rhomboid proteases were described in two papers in 2005 by Lemberg et al. and Urban & Wolfe. Lemberg et al. found that bacterial rhomboid proteases retain activity when solubilized in triton X-100 and DDM, but not in CHAPS [22]. Urban and Wolfe reported activity in DDM and digitonin, but not in triton X-100 and CHAPSO [23]. The reason for the discrepancy in the results with triton X-100 is unclear, but it may be substrate specific, as the two studies utilized different model substrates (derived from drosophila substrates Gurken or Spitz, respectively). A slight activity was detected in nonyl-glucoside, but not in glucosides with shorter alkyl chains [23], indicating that long alkyl chains are necessary to preserve rhomboid activity. Lower activity in detergents with shorter alkyl chains has been confirmed by others, however alkyl chains longer than twelve carbon atoms do not lead to a further increase in activity [25,34,35].

Before crystallizing the glutamyl IMP Rce1, Manolaridis used more than 15 different detergents to screen for the best solubilization efficiency as well as sample monodispersity. The most favorable detergent turned out to be undecyl maltoside (UDM; Fig. 2C). Purified Rce1 also showed enzymatic activity in this detergent, as monitored by a farnesylated model peptide [19]. It must be mentioned, however, that the determination of the Rce1 crystal structure benefited most from the crystallization together with a monoclonal antibody.

### 2.2. Bicelles

Bicelles are artificial planar bilayers with edges stabilized by detergents [36]. They are formed upon mixing particular lipids and detergents, the distinct combination of which defines the properties of the resulting bicelles. The most frequently used pair is dimyristoyl-sn-glycero-phosphocholine (DMPC), a long chain phospholipid, and dihexanoyl-sn-glycero-phosphocholine (DHPC), a short chain phospholipid detergent (Fig. 2D). The two descriptors of bicelle composition are the molar ratio of lipid molecules over detergent molecules (q) and the level of hydration, which is the ratio between added lipid and detergent weight in respect of the total sample weight [37].

The reconstitution of proteins in bicelles is a straightforward, usually hassle-free procedure. Typically it consists of mixing the desired long chain lipid with the detergent of choice and letting the mixture hydrate at room temperature for a specific time, determined by the *q* value. Next, a previously purified solubilized protein is added to the bicelles, usually in a 2:1 volume ratio. Recently, milder reconstitution procedures have been reported, which aim to better preserve the proper protein structure and function [38]. Inevitably, in all cases, a prior isolation and purification of the desired protein will be needed.

Rhomboids have been reconstituted in bicelles in order to study their structure either by X-Ray crystallography, in the case of *E. coli* GlpG in CHAPSO:DMPC [39], or by NMR, in the case of *P. aeruginosa* GlpG in DHPC:DMPC [25] (see Section 3.2 about structural studies). In this last work, the capacity of PaGlpG to cleave a substrate was assessed using a gel based assay for a range of detergents and two bicelle systems. The authors found that rhomboid activity is high in non-ionic detergents – namely DDM (77% substrate cleavage) and NG (45% substrate cleavage), and less pronounced in the ionic and zwitterionic detergents LMPC and LPPG (Fig. 2E). When in bicelles, the proteolytic level was similar to that obtained for nonyl glucoside (NG; Fig. 2F). In recent work, Lemieux and co-workers compared catalytic efficiencies of 3 rhomboids (*E. coli* GlpG, *H. influenzae* GlpG and *P. stuartii* Aara) in DDM detergent micelles or in DMPC bicelles by using an artificial peptide substrate [40]. Interestingly, the catalytic efficiency ($k_{cat}/K_m$) was 4-fold higher for HiGlpG in detergent than in bicelles, whereas it was 4-fold and 58-fold lower for EcGlpG and PsAarA, respectively. This example illustrates the different dependencies of rhomboids on their surroundings.

For aspartyl IMPs, only the presenilin homolog of the archaea *M. marisnigri JR1* has been reconstituted in bicelles. With an artificial renin FRET substrate, Lieberman and co-workers did not find a substantial difference in the catalytic turnover in micelles versus bicelles [24]. However, with a FRET substrate based on the natural APP substrate, substrate affinity was higher in bicelles than in micelles (i.e. $K_m$ in bicelles is lower) [41].

### 2.3. Liposomes

Liposomes are spherical vesicles with one lipid bilayer (unilamellar liposomes; Fig. 1F) or multiple bilayers (multilamellar liposomes) surrounding an aqueous core. Their size ranges from 30 nm to several μm in diameter. Generally, reconstitution of membrane proteins into liposomes is achieved by using the protocol as follows [42]: preparation of unilamellar liposomes from lipids, addition of detergent and a purified membrane protein in micelles to these liposomes, leading to mixed lipid-protein detergent micelles, and subsequent removal of detergent monomers until below the cmc, finally yielding proteoliposomes. Note that his protocol first needs solubilization and purification of the membrane protein of interest in a micelle environment.

Removal of detergent monomers from mixed lipid-protein detergent micelles can be achieved by various methods. These include: (1) Addition of polystyrene beads (“Bio-Beads”), to which detergent will adsorb. This is a preferred method as it most efficient in the removal of detergent. (2) Gel filtration. (3) Dialysis. (4) Dilution. (5) Addition of cyclodextrins that capture detergent monomers. Note that dialysis and gel filtration remove detergent monomers of detergents with high cmc values. In the case of detergents with very small micelle sizes, such as CHAPS (6 kDa micelle size), both detergent monomers and empty micelles may be removed by dialysis and gel filtration. Naturally, when using the dilution strategy, the detergent needs to be diluted to a concentration under the cmc. The highly diluted proteoliposomes can then be concentrated by using density gradient centrifugation, a step that is recommended in any reconstitution in order to separate liposome incorporated target protein from non-incorporated or aggregated protein.

The dependence of γ-secretase on the presence of certain lipids such as phoshatidyl choline (PC) was already observed in experiments using micelles [33]. To investigate the influence of the lipid composition on γ-secretase more thoroughly, the laboratories of Selkoe and Wolfe reconstituted the γ-secretase complex in liposomes of varying compositions [26]. CHAPSO-solubilized and purified γ-secretase was added to CHAPSO-solubilized lipids, and the detergent was removed by Bio-Beads. It was found that sphingolipids and cholesterol increased activity, whereas phosphatidyl inositol decreased activity. In a follow-up study, the same laboratories looked into more detail at the influence of chain length and saturation of fatty acids on the activity and processivity of γ-secretase. The latter refers to the carboxypeptidase activity after the first endoproteolytic cut, which trims down the amyloid-β (Aβ) peptides and determines whether shorter or longer Aβ species are formed (see also Fig. 5). Again, phosphatidylinositol was found to inhibit γ-secretase activity, whereas long fatty acids in phosphatidyl choline (increased membrane thickness) enhanced activity and also processivity, reducing the formation of longer Aβ species [43]. Steiner and co-workers also found that the membrane thickness affects the activity and processivity, with optimal activity in phosphatidyl choline with chainlengths of 18 or 20 carbon atoms. Interestingly, there was no correlation between activity and processivity, as the latter kept increasing with fatty acid chain lengths above 20 carbon atoms [44]. The laboratories of Wolfe and Selkoe further studied the processivity of γ-secretase in liposomes and found evidence for three distinct binding pockets in the primed site of the enzyme, providing a model for the proteolysis of the amyloid precursor protein in three amino acid residue increments [45].

In 2013, Dickey et al. used the rapid dilution method and pelleting by ultracentrifugation to isolate liposomes incorporating different bacterial rhomboid proteases and a fluorescein isothiocyanate (FITC) labeled derivative of the substrate TatA [27]. To prevent that substrate cleavage would already occur before or during the formation of proteoliposomes, they prepared the proteoliposomes at pH 4.0, where rhomboid proteases are inactive, and then shifted the pH to 7.4 to start intramembrane proteolysis. Cleavage experiments revealed that rhomboid proteases display low substrate affinity and process substrates very slowly (in the timescale of minutes). To circumvent problems with premature substrate cleavage during reconstitution, our laboratory has used activity-based probes (ABPs) to label active rhomboids in liposomes [46]. ABPs are small molecule probes that specifically detect active proteases or other enzymes, based on a covalent, mechanism-based reaction with active site residues, thereby linking the enzyme to a tag for read-out [47]. Liposomes themselves were formed using the dialysis method and sizes of approximately 100 nm were verified by dynamic light scattering and transmission electron microscopy. Moreover, giant unilamellar vesicles (approximately 5–10 μm) were imaged by using a fluorescent ABP, illustrating the possibility of activity-based fluorescent microscopy [46].

### 2.4. Amphipols

Amphipols are amphipatic polymers that can act as surfactants for membrane proteins once these are extracted from the lipid bilayer [48]. The use of these polymeric structures requires a two-step procedure: extraction of the membrane protein of interest from its native membrane, usually by detergents and then replacement of the detergent by the amphipol, which now will keep the protein soluble in aqueous media via non-covalent interactions with the protein surface [49]. The multiple attachment points of the amphipols with the transmembrane domain of the protein ensure the maintenance of the amphipol-protein interaction, which will only be displaced if another surfactant with higher affinity is present in the media [50].

In order to create protein-amphipol complexes, a concentrated aqueous solution of amphipol is added to the membrane protein solubilized in detergent. The amphipols will readily partition into the detergent micelles, forming ternary complexes that consist of protein, detergent and amphipol. Noteworthy, these complexes will also accommodate lipids if present in the media. Finally, the micelles are removed, which can be done by various methods. The two most commonly used methods [51] are: (1) diluting the sample under the cmc of the detergent or (2) dialysis in the presence of polystyrene beads (Biobeads SM2) which will remove the detergent present in the media.

The most widely used amphipol is A8-35 (see Fig. 1E). Shi and co-workers used A8-35 to solubilize γ-secretase and eliminate the detergent which interfered with data acquisition in cryo-EM. This change brought high resolution γ-secretase structure determination in cryo-EM [28,52].

### 2.5. Lipid nanodiscs

Lipid nanodiscs are nanometer sized pieces of lipid bilayer stabilized by a polymeric agent. Two types of stabilizing entities have been reported in literature: protein polymers, better known as membrane scaffolding proteins (MSPs) [53] and copolymers based on maleic acid (xMA) [54,55].

MSPs are amphipathic α-helical proteins typically derived from the human apolipoprotein A1. Two of these proteins form a stabilizing belt around lipids, forming a nanodisc shaped lipid bilayer [56]. The formation of MSP nanodiscs always requires the use of detergents because the MSPs, despite being surfactants, are not able to disrupt biological membranes. There are two methods to prepare these nanodiscs: (1) It is most common to use a previously purified protein in a detergent micelle. Externally supplied lipids and MSPs followed by detergent removal will then lead to nanodiscs. Although this system allows a customized size of the nanodisc and a controlled lipid content, information about the native lipid environment around the membrane protein is inevitably lost. (2) Sligar and co-workers have reported the application of detergent and MSP to crude membranes in order to solubilize a membrane protein of interest [57]. Subsequent detergent removal allowed the formation of MSP discs, in which the native lipids will be included.

xMAs are amphipathic copolymers of maleic acid and styrene (SMA; also known as Lipodisq®) [58] or diisobutylene (DIBMA) [59]. These polymers are able to directly extract and solubilize membrane proteins and their associated native lipids from crude membranes, forming native lipid nanodiscs. Remarkably, this approach is the only one that allows the preservation of the native lipids around the membrane protein as it by-passes the use of detergent. In addition, membrane proteins that are instable in detergent, can now directly be solubilized in a lipid environment, in contrast to bicelles, liposomes and MSP-stabilized nanodiscs.

Whereas MSP lipid nanodiscs remain unused in the IMP field, xMA solubilization has recently been used for rhomboid proteases [29,60–62]. To date only the *E. coli* GlpG and the *V. cholerae* rhomboid have been solubilized in either SMA or DIBMA. As shown in these first studies, the IMPs in native nanodiscs systems are compatible with activity assays [29,60] and techniques such as hydrogen-deuterium exchange mass spectrometry [29] or laser-induced liquid bead ion desorption mass spectrometry [61]. Importantly, the unstable *V. cholerae* rhomboid, which rapidly self-processes in detergent micelles, is stable and functionally active in xMA stabilized lipid nanodics [60]. Hence, these systems promise to also offer an increased stability of the IMP and a more native like environment in comparison with other solubilization techniques.

## 3. Applications

The available diversity of methods to isolate IMPs in different mimetics of the biological membrane, as discussed in Section 2, allows the detailed analysis of IMPs in different types of studies. In Section 2, we have already discussed the influence of different lipids or other

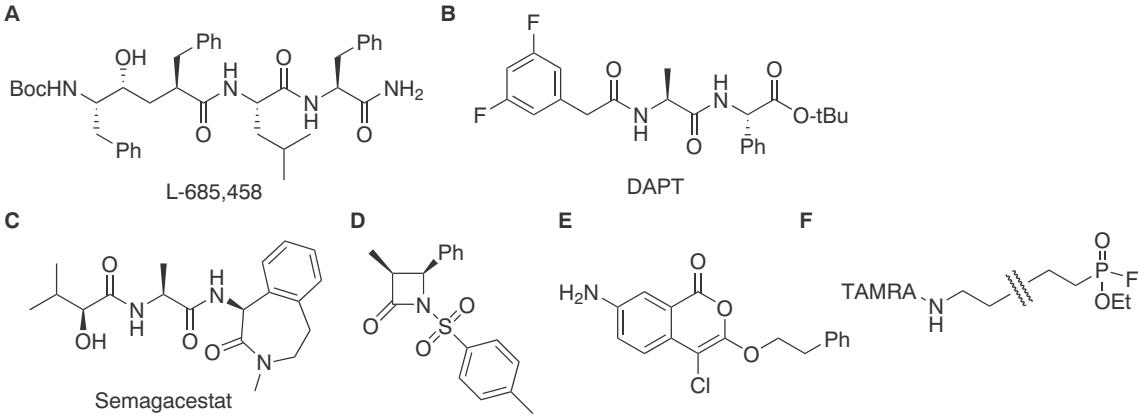


**Fig. 3.** Chemical structures of small molecules targeting γ-secretase (A–C) and rhomboid proteases (D–F). (A) L-685,458 (also known as inhibitor X) is a transition state analog inhibitor of γ-secretase. (B) DAPT is an inhibitor of γ-secretase with a different binding site than L-685,458. (C) Semagacestat advanced to phase III clinical trials as a γ-secretase inhibitor, however due to its severe toxicity, the trials were discontinued. (D) N-sulfonylated-β-lactams have been reported as potent, covalent inhibitors of bacterial rhomboid proteases. (E) A 4-chloro-isocoumarin derivative with submicromolar activity against EcGlpG. (F) FP-Rhodamine is a general serine hydrolase ABP. It contains a fluorophosphonate group as electrophilic warhead, which covalently reacts with the active site of serine hydrolases, including rhomboid proteases.

hydrophobic environments on the activity of IMPs. In this section, we will specifically focus on inhibition assays, structural studies and some functional studies.

### 3.1. Inhibition assays

For site-2 protease, very few inhibitors are currently described and we are unaware of any systematic inhibitor screening for this family of IMPs. Clearly, there is still a gap to be filled, and the availability of solubilized and purified S2P may aid the discovery of novel S2P inhibitors. The discovery of Rce1 inhibitors has traditionally made use of yeast membranes overexpressing Rce1 instead of isolated protein, which is also high throughput screen compatible [63]. For the discovery of γ-secretase inhibitors, inhibitor assays had been performed long before the protease complex was purified and even before the catalytic and other subunits were discovered. A compounds screen on cells, measuring Aβ formation with a homogeneous time-resolved fluorescence (HTRF) immuno assay, identified the transition state analog L-685,458 (Fig. 3A) as a potent γ-secretase inhibitor [64]. Interestingly, this compound formed the basis for one of the studies identifying presenilin as the protease component of γ-secretase [13]. Elan Pharmaceuticals and Eli Lilly & Company reported a cellular high throughput screen of 25,000 compounds using a sandwich ELISA [65]. This finally resulted in the inhibitor DAPT (Fig. 3B) and derivatives such as Semagacestat (Fig. 3C), which unfortunately failed in clinical trials [66]. Overall, most inhibitor studies for γ-secretase have not benefited from solubilization and purification of the γ-secretase complex. Since several years, γ-secretase targeting drug discovery for Alzheimer's disease has shifted from inhibitors to modulators, which do not block proteolytic activity, but alter the carboxypeptidase activity to produce shorter, less toxic Aβ species.

The first work describing detergent solubilized and purified bacterial rhomboids revealed that the most commonly used general serine protease inhibitors are not or only very poorly active [22,23]. Efficient inhibition could only be achieved with high concentrations of 3,4-dichloroisocoumarin, and to lesser extent *N*-tosyl-phenylalanine chloromethylketone (TPCK). High concentrations of such covalent inhibitors may show general cellular toxicity effects. Hence, in contrast to γ-secretase, for rhomboids the development of in vitro assays was desirable.

The first HTS for rhomboid proteases was reported by Freeman and co-workers, who made use of detergent solubilized and purified *P. stuartii* rhomboid AarA and a quenched fluorescent peptide substrate based on the TMH of *Drosophila* substrate Gurken [67]. The activity or inhibition was measured in a fluorescence endpoint assay. After screening 58,000 small molecules, *N*-sulfonylated β-lactams (Fig. 3D) were discovered as novel type of inhibitor. To circumvent the use of a fluorescently labeled substrate, Vosyka et al. developed a MALDI-TOF mass spectrometry based assay, which monitored cleavage of the purified recombinant model substrate TatA [34]. New 4-chloro-isocoumarin derivatives with submicromolar potency were found (Fig. 3E). The discovery of ABPs for rhomboid proteases [68], which are able to fluorescently modify the protease active site in a mechanism based reaction, allows substrate-free inhibition assays. This is beneficial, because the substrate specificity of rhomboid proteases is still ill-defined and no general substrate for activity read-out has been reported. The ABP FP-Rhodamine (Fig. 3F) is a pan reactive rhomboid probe, which allows either gel-based inhibitor screening [69] or inhibitor screening using activity-based fluorescence polarization [70]. Importantly, the potency of rhomboid protease inhibitors was not substantially affected by the environment as reported for micelle versus liposome embedded *E. coli* GlpG, confirming that micelle-solubilized rhomboids are a good model system for inhibitor discovery [46].

### 3.2. Structure elucidation

Structures of IMPs have provided invaluable information regarding the catalytic mechanism, the recognition of substrates and – to much lesser extent – the interaction with lipids. Most of these have used X-ray crystallography. The higher degree of structural complexity of the multimeric γ-secretase demanded the utilization of cryo-EM. Regardless of the method, a stable and homogeneous conformation of the target IMP is required. Hence, the selection of an appropriate reconstitution method is essential. We here classify the structural studies with regards to the presence or absence of IMP interaction partners.

#### 3.2.1. Structural insights into the apo-enzyme

The rhomboid EcGlpG was the first IMP structure solved at atomic resolution. Ha and co-workers produced crystals from a solution of the GlpG transmembrane core in NG detergent micelles. The structure confirmed the previously predicted 6 TMHs and revealed a water filled cavity opened to the extracellular space [71]. Almost simultaneous with this work, three different research groups reported structures of GlpG from *E. coli* [72,73] or its *H. influenzae* homolog [74].

Shortly after the initial structures of GlpG, Shi and co-workers reported the first crystal structure of a metallo IMP, the S2P of *M. jannaschii* [75]. Although purified in decyl-maltoside micelles, two

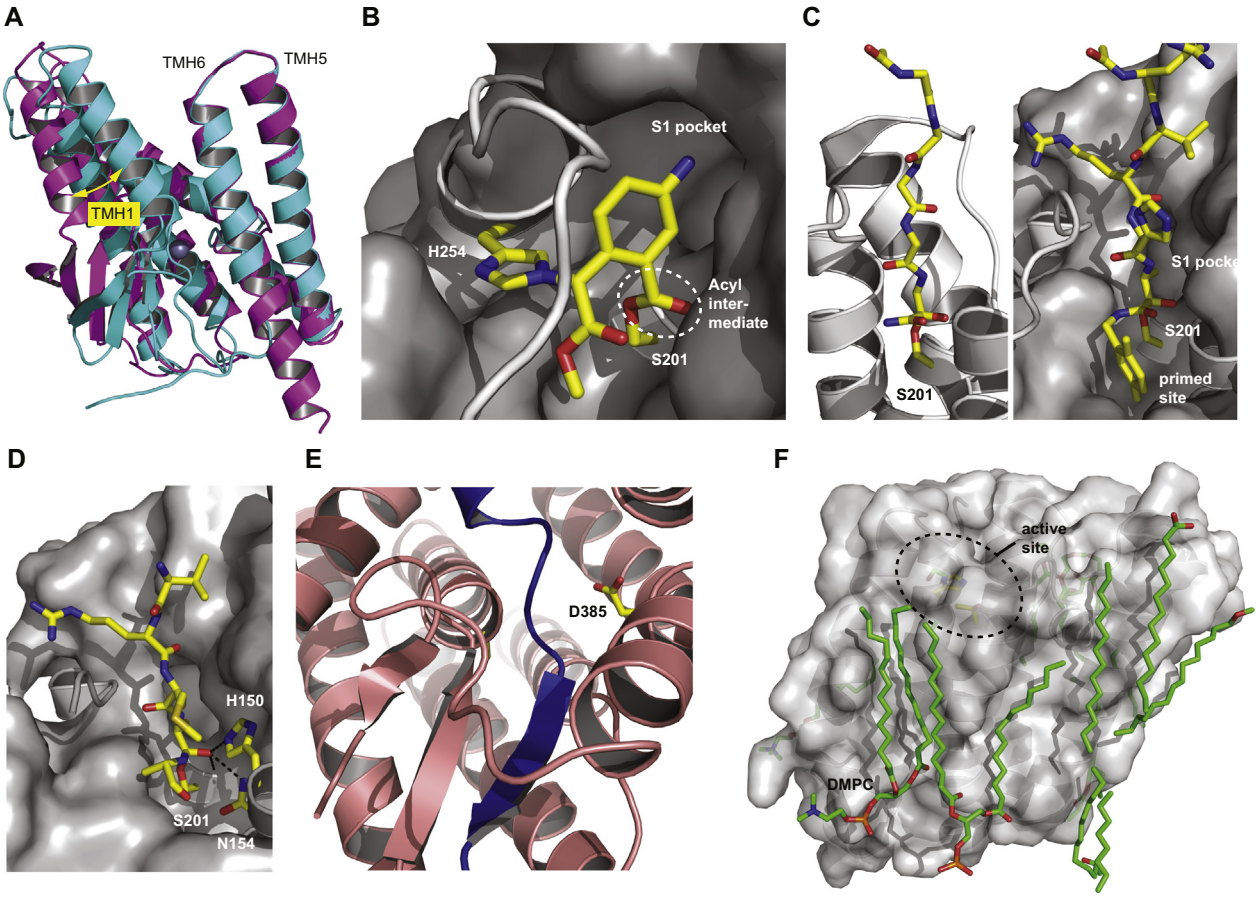


**Fig. 4.** Structural information on IMPs. (A) Superimposition of S2P crystal structures in open (magenta) and closed conformation (blue). The lateral displacement of TMH1 can be observed; the rest of the structure remains practically identical in both conformations (PDB code: 3B4R) (B) Co-crystal of *Ec*GlpG with an isocoumarin inhibitor in its active site. The complex is trapped in the acyl-enzyme intermediate form, essential for proteolysis. The S1 pocket in the enzyme and its catalytic dyad, formed by the residues H254 and S201 are indicated. (PDB code: 2XOW) (C) A peptidyl ketoamide inhibitor (in stick representation) covalently bound to the S201 of *Ec*GlpG (PDB code: 5MTF), depicted in cartoon mode. In the left panel, the β-strand character of the peptide backbone can be seen. For clarity, the side chains and primed site of the inhibitor are omitted. The right panel shows how the inhibitor binds to the S1 pocket and the primed site. Note that for clarity, not all residues are included in the surface representation of the enzyme. (D) Crystal structure (PDB code: 6PJA) of a substrate-rhomboid tetrahedral intermediate. The substrate is bound to active site serine S201. The oxygen of the tetrahedral intermediate makes contacts (indicated with black dotted lines) to the oxyanion hole formed by H150, N154 and the backbone of S201. (E) Cryo-EM structure of γ-secretase with its substrate APP (in blue) in the binding cleft. It shows the transition from a α-helix to a β-strand that the substrate must undergo before it can be cleaved by γ-secretase. (PDB code: 6IYC) (F) Crystal of the inactive mutant of *Ec*GlpG (in grey) in a bicelle. In this structure we can see how annular DMPC lipids (in stick representation) are fitting their acyl chains (in green) into the grooves of the protein. The active site of the protease is encircled, for clarity (PDB code: 2XTV).

additional detergents were added to the crystallization buffer to improve the crystal diffraction properties. Remarkably, in the obtained crystals the S2P appears trapped in two conformations in which TMH1 and TMH6 move 10–12 Å apart. The authors suggest that these are the open and closed conformations, which provide a lateral gating mechanism to grant a substrate access to the active site (Fig. 4A).

In 2011, Ha and co-workers solved the first structure of an aspartyl IMP, the preflagellin protease FlaK of *M. maripaludis*, which was crystallized from cyclohexylhexylmaltoside micelles [76]. The crystal structure revealed that FlaK is not perpendicularly oriented to the plane of the membrane but titled and in an inactive conformation with the two catalytic aspartates at a 12 Å distance. FlaK has only 6 TMHs, whereas SPP and the PS subunit of γ-secretase have 9. The first structure of an aspartyl IMP with 9 TMDs was that of the PS homolog of *M. marisnigri JR1*, crystallized from nonylmaltoside micelles [77]. In 2013, the latest catalytic family of IMPs was crystallized: *M. maripaludis* Rce1, a glutamyl IMP [19]. In order to aid crystal formation, Rce1 was co-crystalized with an antibody.

As expected, the structural elucidation of the complete γ-secretase complex was a more challenging task than for IMPs consisting of a single protein chain. Biochemical studies, including detergent-mediated dissociation (see Section 2.1), shed some light on the structural organization of the γ-secretase complex. Various low resolution structures using negative stain electron microscopy and cryo-EM started to reveal the shape of the protease complex. For a summary of these studies, we would like to refer to a specialized review on this topic [78].

The use of amphipols, which minimizes the effects of disordered detergent and leads to better image reconstruction, led to the elucidation of the γ-secretase structure at 4.5 Å by cryo-EM [28]. The study showed a horseshoe shaped structure and detected 19 TMHs – with a later report by Sun et al. revealing all 20 TMHs [79]. Follow-up work, employing amphipols and improved data acquisition parameters, finally led to a structure with atomic resolution [52]. Contrary to what was expected, the active site residues were located at the convex side of the horseshoe structure (Fig. 1B).

Overall, the use of detergents and amphipols in X-ray crystallography and cryo-EM has proven instrumental for the elucidation of structural features of IMP apoenzymes.

### 3.2.2. Substrate interaction with IMPs

The first structural insights into the interaction between IMPs with substrates came from rhomboid proteases in complex with covalent

inhibitors. In 2010, Vinothkumar et al. reported GlpG in complex with an isocoumarin [80], which allowed observing the acyl intermediate of GlpG and unambiguously identify the S201 as the reactive nucleophile. The inhibitor bound structure also revealed the potential S1 pocket (Fig. 4B). The structural differences with the apoenzyme were minor, suggesting that the changes GlpG undergoes during catalysis are only subtle. Since then, various other rhomboid inhibitors and their crystal structures have followed [81]. The recently reported reversible covalent peptidyl ketoamide inhibitors are particularly interesting, as they interact with both primed and non-primed site and span from the P4 position to the P2′ position [82]. Therefore, they potentially represent a substrate in a closer way than previous rhomboid-inhibitor structures. X-ray crystallography with these inhibitors revealed that the peptidic moiety in the non-primed site binds as an extended β-strand, whereas the non-peptidic binding element at the other side of the ketoamide occupies a hydrophobic pocket in the primed site (Fig. 4C). An overlay with crystal structures containing other inhibitors revealed that this site is quite malleable and can adapt to substituents of various sizes. A recent report by the Urban laboratory described the use of time-resolved X-ray crystallography of GlpG in a bicelle in the presence of a substrate peptide of 13 amino acid residues [83]. Soaking crystals with peptide substrate for various amounts of time before flash freezing and X-ray diffraction allowed the visualization of distinct steps in the catalytic cycle. Surprisingly, the tetrahedral intermediate could be observed, suggesting that this intermediate is relatively stable through interactions with H150, N154 and the backbone of S201 (Fig. 4D). The conformation of the substrate within the tetrahedral intermediate shows remarkable similarities with the ketoamide inhibitor structure, as both bind in a beta-strand-like manner (Fig. 4C and D). The different snapshots also revealed that TMH5, previously implied as lateral gate, becomes unstructured upon interaction with the substrate. Loop L5 that caps the active site, was known to be mobile in order to grant inhibitors and substrates access to the active site. Here, however, it was shown that this loops clamps back onto the substrate after entry and plays a role in substrate processing.

Recently, two structures of γ-secretase in complex with the TMH of Notch [84] or APP [85] were reported, both solved by cryo-EM in mixed 0.1% digitonin/1% CHAPSO micelles. To avoid substrate cleavage, a catalytically inactive D385A mutant of PS1 was used. The structures revealed pronounced conformational rearrangements in parts of PS1 and substrates. Notably, the carboxyterminal end of the substrate helix forms a β-sheet with two β-strands of PS1, which are formed upon substrate binding (Fig. 4E). Although it was already apparent that substrate helices need to unwind before cleavage, the γ-secretase structures, the peptidyl ketoamide inhibitor-bound rhomboid and the substrate-bound rhomboid structure showcase that similar conformational changes from a helix to an extended β-strand are required for access of the catalytic machinery to the scissile bond.

#### 3.2.3. Lipid interactions with IMPs

As discussed in various examples in Section 2, the membrane environment can affect the stability or activity of IMPs, yet a structural understanding of the mechanisms by which lipids exert an influence on IMPs is still lacking. What is thus far known about the structural interaction of lipids and IMPs?

Various crystal structures of rhomboid proteases have revealed the presence of lipids. Lemieux et al. describe three lipid molecules in the structure of HiGlpG, putatively phosphatidic acid (PA): two flanking loop L1 and the third localized near TMH6 [74]. Ben-Shem et al. found a phospholipid in the structure of EcGlpG, entering the active site between TMH2 and TMH5, with the phosphate group hydrogen bonding to various residues [73]. The role and significance of these lipids, however, remain unclear.

Vinothkumar used DMPC/CHAPSO as reconstitution system to solve the EcGlpG structure in a bicelle [39]. Here, 14 ordered lipid molecules were identified, the majority being annular lipids with their acyl chains fitting into grooves of the protein structure (Fig. 4F). More interestingly, upon comparison of GlpG in a bicelle with its delipidated homolog in a micelle, the structural differences proved to be minimal and exclusively occurred in specific residues of L5. Remarkably, in the micelle, some detergent molecules occupied the positions of the previously mentioned annular lipids. These findings prove that – at least for GlpG – particular detergents form a good mimic for lipids [39].

Also γ-secretase structures have detected the presence of lipid molecules. In the first atomic structure of the γ-secretase complex, Bai et al. identified two phospholipids present at the interfaces of PS1/Aph-1 and Nct/Aph-1. It was speculated that these ordered lipids may have a stabilizing function for interaction with the membrane [52]. In the recent substrate-bound γ-secretase cryo-EM structures, different lipids were also observed. In the Notch-complexed structure, four PC molecules were found to stabilize PS1 interfaces with other subunits. In addition, three cholesterols were detected binding the hydrophobic surface of Aph-1 [84]. In the APP-complexed structure, three cholesterol molecules are also present. However, in this case only 2 PC molecules were detected [85].

Unlike the IMP structures with substrates or inhibitors, which revealed detailed functional features, the current insight into the lipid-IMP interactions is clearly still in its infancy. We believe that performing structural and functional studies in the same reconstitution system will be critical in order to reveal the importance of these interactions on function.

### 3.3. Other functional studies

Besides inhibitor discovery and structural insights, solubilization and purification of IMPs has also yielded a wealth of functional information on the different IMP families. Below, we selected a number of particularly interesting recent studies that led to novel biochemical and biological insights by using IMPs in various membrane mimicking environments.

Two subunits of the γ-secretase complex come in two different forms: presenilin (PS1 and PS2), and Aph-1 (Aph1a and Aph1b), which enables the formation of four different complexes. The laboratory of De Strooper and Chavez-Gutierrez isolated all of these complexes by overexpression in insect cells, CHAPSO-solubilization and purification by a GFP-tag on the Nct subunit [86]. It turned out that the composition of the γ-secretase complex affects both endopeptidase and carboxypeptidase activity. Particularly, complexes with PS2 display lower endopeptidase activity than those with PS1, but the position of this first ε-cut is similar in both. However, the subsequent processing by the carboxypeptidase activity is different: in PS2 containing complexes, the production line resulting in Aβ42 and Aβ38 (see Fig. 5) is less favored with respect to that resulting in Aβ40. In addition, Aph1b containing complexes display a less efficient carboxypeptidase activity than those with Aph1a [86]. Overall, this adds an extra layer of complexity to the formation of toxic Aβ production, but it may also be exploited in therapeutic targeting of specific γ-secretase complexes.

What is the underlying mechanism of formation of longer, more toxic Aβ peptides in Alzheimer's disease? An explanation was recently provided by Chavez-Gutierrez and co-workers by looking at the stability of enzyme-substrate complexes with purified recombinant γ-secretase and APP in detergent micelles [87]. Pathogenic mutations in both PS and APP lead to a destabilized interaction between the enzyme and the substrate, which results in dissociation of the substrate before the final carboxypeptidase cut. As a consequence, longer Aβ-species are formed. Importantly, this work provides a new viewpoint for the development of drugs against Alzheimer's disease, namely the development of compounds that stabilize the enzyme-substrate interaction [87].

How rhomboid proteases are regulated in their activity is largely unknown. The presence of two $Ca^{2+}$-binding “EF-hands” in the cytosolic domain of *Drosophila* rhomboid-4 (DmRho4) attracted the attention of the Urban laboratory. Experiments in cell culture, but also with

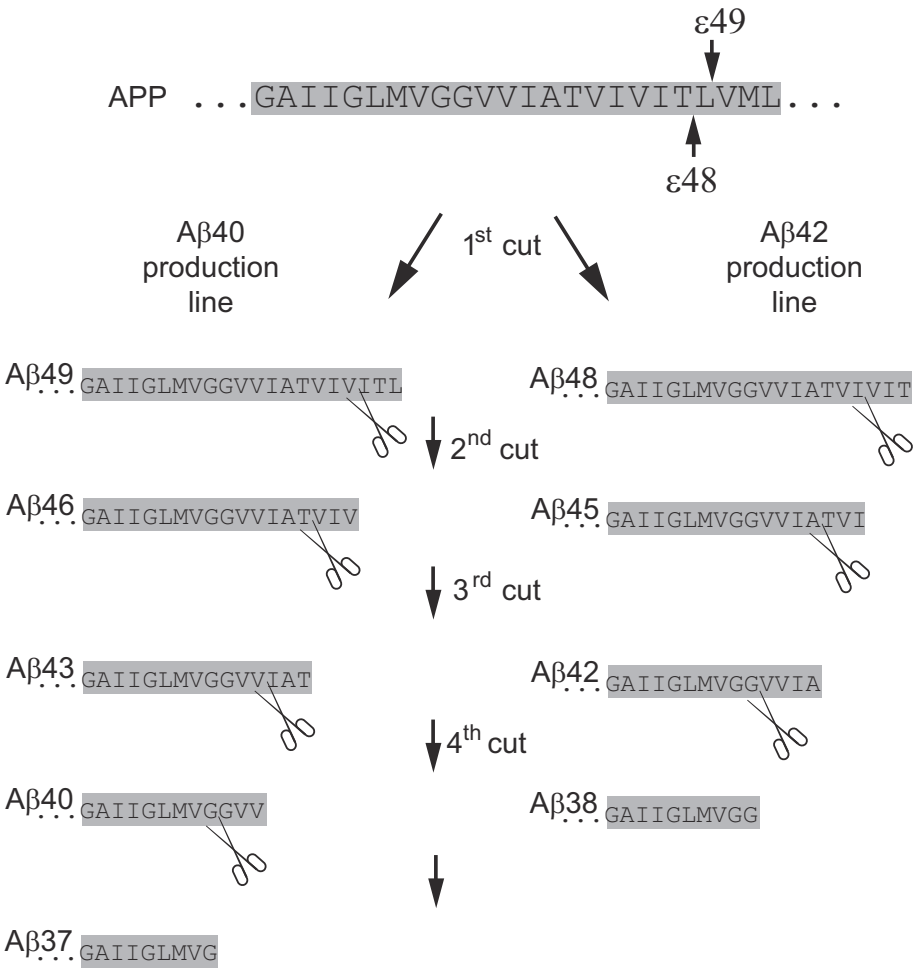


**Fig. 5.** Schematic representation of the sequential cleavages of APP by γ-secretase. A first endoproteolytic cut (ε) can happen at two different positions. Eventually, this determines whether the Aβ40 or Aβ42 "production line" is followed. After the first cut, several sequential carboxypeptidase cleavages take place, trimming down the Aβ peptide. Depending on the stability of the enzyme-substrate complex, the Aβ peptide may be released from the enzyme before it reaches the end of the production line, leading to longer or shorter Aβ species that display different toxicities.

purified, liposome reconstituted DmRho4, revealed that $Ca^{2+}$ stimulates proteolysis of substrates [88]. The activation effect was even larger on mutants lacking the cytosolic domain, pointing at an inhibitory effect of the EF hands and the presence of another $Ca^{2+}$ binding site that activates proteolysis. Several residues in cytosolic loops 4 and 6 were identified as important for this activation effect. A concomittant shift to cleavage sites deeper into the membrane led to a model of activation, in which $Ca^{2+}$ binding to the cytosolic loops results in better lateral access of substrates into the active site [88].

Recently, Urban and co-workers used single-molecule total internal reflection fluorescence (smTIRF) microscopy for single particle tracking of various rhomboid proteases in cells and in planar supported lipid bilayers, generated from rhomboid-containing liposomes [89]. Rhomboid proteases diffused through the membrane faster than other membrane proteins and, astoundingly, faster than the viscosity of the membrane should allow for a protein of this size. The remarkably rapid diffusion of rhomboid proteases was attributed to the size of the rhomboid's hydrophobic core, which is thinner than the hydrophobic core of the membrane surrounding the rhomboid. Resolving this hydrophobic 'mismatch' with thinner lipid bilayers, which usually increase diffusion, actually slowed down the rate of rhomboid diffusion. Overall, the hydrophobic mismatch plays a role in rhomboid diffusion and ultimately its catalytic turnover of substrates [89].

Little is known about the effect that the lipid environment exerts on the structure of IMPs. Reading et al. used hydrogen-deuterium exchange mass spectrometry to study GlpG in xMALPs of diverse lipid compositions [29]. Changes in the relative abundance of the lipid headgroups did not have a significant effect on GlpG structural dynamics. Interestingly, upon increasing the degree of lipid tail unsaturation, TMH1 of GlpG and the cytoplasmic domain linker region appeared to be more exposed to the hydrophilic environment.

## 4. Conclusion and future directions

Intramembrane proteolysis is an intriguing and biologically important process. Numerous studies have helped us understand the biochemical mechanisms of IMPs and further clarify their biological roles. It is now possible to reconstitute IMPs in several different membrane mimicking environments and purify them to high homogeneity. Whereas all catalytic types of IMPs have been solubilized with detergent micelles, other systems such as bicelles and lipid nanodiscs have only been applied to a few families. Hence, there is a lot of room for future research. We expect that the experience in reconstitution methods for one IMP family may be directly transferred to other catalytic types.

The lipid environment seems to have a pronounced effect on the activity and stability of IMPs. However, a systematic investigation of the influence of different lipid species on IMP activity has only been reported for γ-secretase in studies that varied the lipid composition of liposomes in which γ-secretase was reconstituted (see Section 2.3).

Although these experiments are not easy to carry out, it will be worth performing similar studies on other IMP families.

Due to the involvement of IMPs in various pathological processes, IMPs are potential drug targets [7]. Most drug discovery has thus far been performed for γ-secretase because of its link with Alzheimer's disease. Unfortunately, both GSIs and GSMs have failed in clinical trials [8]. Nevertheless, various GSIs are currently in clinical trials for cancer treatment. Inhibitors may also be used as tool compounds to further unravel the cellular role of IMPs. Clearly, such inhibitors would need to be cell permeable, highly selective and non-toxic. The recently reported peptidyl ketoamide inhibitors of rhomboid proteases seem to fulfil these criteria [82], but for other IMP families, such as S2P, selective inhibitors are still missing. The ability to solubilize and purify IMPs will support future screening for and development of inhibitors for these families as well.

The last decade has seen the elucidation of structures with atomic details for all four different catalytic types of IMPs. However, there is still a lot to learn. For rhomboid proteases, for example, only structures of GlpG, which has a 6 TMH core, have been solved. Various mammalian rhomboids have an additional N- or C-terminal TMH, which likely will display differences that could be crucial for substrate recognition and/or inhibitor development. The interaction of IMPs with their substrates has been inferred from inhibitor-rhomboid structures. Only recently, the first true substrate-protease complexes were reported for γ-secretase and rhomboid GlpG, revealing details of substrate helix unwinding.

To gain a larger structural understanding of the functional interaction between IMPs and lipids, there is a pressing need for methods that capture ordered lipids at the edges of these membrane embedded proteases. We expect that solubilization methods such as xMALPs or MSP-stabilized lipid nanodiscs in combination with cryo-EM may facilitate such studies.

## Declaration of competing interest

The authors declare no conflict of interest.

## Acknowledgments

We thank financial support by H2020 (Marie Curie Individual Fellowship to MBX), Stichting Alzheimer Onderzoek, the Ministerium für Kultur und Wissenschaft des Landes Nordrhein-Westfalen, the Regierende Bürgermeister von Berlin–inkl. Wissenschaft und Forschung, and the Bundesministerium für Bildung und Forschung.

## References

[1] R.B. Rawson, N.G. Zelenski, D. Nijhawan, J. Ye, J. Sakai, M.T. Hasan, T.Y. Chang, M.S. Brown, J.L. Goldstein, Mol. Cell 1 (1997) 47–57.
[2] H. Beard, M. Barniol-Xicota, J. Yang, S.H.L. Verhelst, ACS Chem. Biol. 14 (2019) 2372–2388.
[3] D. Avci, M.K. Lemberg, Trends Cell Biol. 25 (2015) 611–622.
[4] R.B. Rawson, Biochim. Biophys. Acta 1828 (2013) 2801–2807.
[5] J.S. Schneider, M.S. Glickman, Biochim. Biophys. Acta 1828 (2013) 2808–2814.
[6] S.E. Hampton, T.M. Dore, W.K. Schmidt, Crit. Rev. Biochem. Mol. Biol. 53 (2018) 157–174.
[7] S.H.L. Verhelst, FEBS J. 284 (2017) 1489–1502.
[8] B. De Strooper, L. Chavez Gutierrez, Annu. Rev. Pharmacol. Toxicol. 55 (2015) 419–437.
[9] L.D. Sibley, Biochim. Biophys. Acta 1828 (2013) 2908–2915.
[10] Y. Akiyama, K. Kanehara, K. Ito, EMBO J. 23 (2004) 4434–4442.
[11] C. Lazareno-Saez, E. Arutyunova, N. Coquelle, M.J. Lemieux, J. Mol. Biol. 425 (2013) 1127–1142.
[12] P.C. Fraering, M.J. LaVoie, W. Ye, B.L. Ostaszewski, W.T. Kimberly, D.J. Selkoe, M.S. Wolfe, Biochemistry 43 (2004) 323–333.
[13] Y.M. Li, M. Xu, M.T. Lai, Q. Huang, J.L. Castro, J. DiMuzio-Mower, T. Harrison, C. Lellis, A. Nadin, J.G. Neduvelil, R.B. Register, M.K. Sardana, M.S. Shearman, A.L. Smith, X.P. Shi, K.C. Yin, J.A. Shafer, S.J. Gardell, Nature 405 (2000) 689–694.
[14] D. Seiffert, J.D. Bradley, C.M. Rominger, D.H. Rominger, F. Yang, J.E. Meredith Jr., Q. Wang, A.H. Roach, L.A. Thompson, S.M. Spitz, J.N. Higaki, S.R. Prakash, A.P. Combs, R.A. Copeland, S.P. Arneric, P.R. Hartig, D.W. Robertson, B. Cordell, A.M. Stern, R.E. Olson, R. Zaczek, J. Biol. Chem. 275 (2000) 34086–34091.
[15] W.P. Esler, W.T. Kimberly, B.L. Ostaszewski, T.S. Diehl, C.L. Moore, J.Y. Tsai, T. Rahmati, W. Xia, D.J. Selkoe, M.S. Wolfe, Nat. Cell Biol. 2 (2000) 428–434.
[16] A. Weihofen, K. Binns, M.K. Lemberg, K. Ashman, B. Martoglio, Science 296 (2002) 2215–2218.
[17] J.R. Lee, S. Urban, C.F. Garvey, M. Freeman, Cell 107 (2001) 161–171.
[18] S. Urban, J.R. Lee, M. Freeman, Cell 107 (2001) 173–182.
[19] I. Manolaridis, K. Kulkarni, R.B. Dodd, S. Ogasawara, Z. Zhang, G. Bineva, N. O'Reilly, S.J. Hanrahan, A.J. Thompson, N. Cronin, S. Iwata, D. Barford, Nature 504 (2013) 301–305.
[20] W.P. Esler, W.T. Kimberly, B.L. Ostaszewski, W. Ye, T.S. Diehl, D.J. Selkoe, M.S. Wolfe, Proc. Natl. Acad. Sci. U. S. A. 99 (2002) 2720–2725.
[21] T. Sato, A.C. Nyborg, N. Iwata, T.S. Diehl, T.C. Saido, T.E. Golde, M.S. Wolfe, Biochemistry 45 (2006) 8649–8656.
[22] M.K. Lemberg, J. Menendez, A. Misik, M. Garcia, C.M. Koth, M. Freeman, EMBO J. 24 (2005) 464–472.
[23] S. Urban, M.S. Wolfe, Proc. Natl. Acad. Sci. U. S. A. 102 (2005) 1883–1888.
[24] S.H. Naing, K.M. Vukoti, J.E. Drury, J.L. Johnson, S. Kalyoncu, S.E. Hill, M.P. Torres, R.L. Lieberman, ACS Chem. Biol. 10 (9) (2015) 2166–2174.
[25] A.R. Sherratt, M.V. Braganza, E. Nguyen, T. Ducat, N.K. Goto, Biochim. Biophys. Acta 1788 (2009) 2444–2453.
[26] P. Osenkowski, W. Ye, R. Wang, M.S. Wolfe, D.J. Selkoe, J. Biol. Chem. 283 (2008) 22529–22540.
[27] S.W. Dickey, R.P. Baker, S. Cho, S. Urban, Cell 155 (2013) 1270–1281.
[28] P. Lu, X.C. Bai, D. Ma, T. Xie, C. Yan, L. Sun, G. Yang, Y. Zhao, R. Zhou, S.H. Scheres, Y. Shi, Nature 512 (2014) 166–170.
[29] E. Reading, Z. Hall, C. Martens, T. Haghighi, H. Findlay, Z. Ahdash, A. Politis, P.J. Booth, Angew. Chem. Int. Ed. Engl. 56 (2017) 15654–15657.
[30] Y.M. Li, M.T. Lai, M. Xu, Q. Huang, J. DiMuzio-Mower, M.K. Sardana, X.P. Shi, K.C. Yin, J.A. Shafer, S.J. Gardell, Proc. Natl. Acad. Sci. U. S. A. 97 (2000) 6138–6143.
[31] W.T. Kimberly, M.J. LaVoie, B.L. Ostaszewski, W. Ye, M.S. Wolfe, D.J. Selkoe, Proc. Natl. Acad. Sci. U. S. A. 100 (2003) 6382–6387.
[32] D. Edbauer, E. Winkler, J.T. Regula, B. Pesold, H. Steiner, C. Haass, Nat. Cell Biol. 5 (2003) 486–488.
[33] P.C. Fraering, W. Ye, J.M. Strub, G. Dolios, M.J. LaVoie, B.L. Ostaszewski, A. van Dorsselaer, R. Wang, D.J. Selkoe, M.S. Wolfe, Biochemistry 43 (2004) 9774–9789.
[34] O. Vosyka, K.R. Vinothkumar, E.V. Wolf, A.J. Brouwer, R.M. Liskamp, S.H.L. Verhelst, Proc. Natl. Acad. Sci. U. S. A. 110 (2013) 2472–2477.
[35] A.C. Foo, B.G. Harvey, J.J. Metz, N.K. Goto, Protein Sci. 24 (2015) 464–473.
[36] C.R. Sanders 2nd, G.C. Landis, Biochemistry 34 (1995) 4030–4040.
[37] U.H. Durr, R. Soong, A. Ramamoorthy, Prog. Nucl. Magn. Reson. Spectrosc. 69 (2013) 1–22.
[38] E.A. Morrison, K.A. Henzler-Wildman, Biochim. Biophys. Acta 1818 (2012) 814–820.
[39] K.R. Vinothkumar, J. Mol. Biol. 407 (2011) 232–247.
[40] E. Arutyunova, Z. Jiang, J. Yang, A.N. Kulepa, H.S. Young, S. Verhelst, A.J. O'Donoghue, M.J. Lemieux, Biol. Chem. 399 (2018) 1389–1397.
[41] S.H. Naing, S. Kalyoncu, D.M. Smalley, H. Kim, X. Tao, J.B. George, A.P. Jonke, R.C. Oliver, V.S. Urban, M.P. Torres, R.L. Lieberman, J. Biol. Chem. 293 (2018) 4653–4663.
[42] J.L. Rigaud, D. Levy, Methods Enzymol. 372 (2003) 65–86.
[43] O. Holmes, S. Paturi, W. Ye, M.S. Wolfe, D.J. Selkoe, Biochemistry 51 (2012) 3565–3575.
[44] E. Winkler, F. Kamp, J. Scheuring, A. Ebke, A. Fukumori, H. Steiner, J. Biol. Chem. 287 (2012) 21326–21334.
[45] D.M. Bolduc, D.R. Montagna, M.C. Seghers, M.S. Wolfe, D.J. Selkoe, Elife 5 (2016).
[46] E.V. Wolf, M. Seybold, R. Hadravova, K. Strisovsky, S.H.L. Verhelst, ChemBioChem 16 (2015) 1616–1621.
[47] S. Chakrabarty, J.P. Kahler, M.A.T. van de Plassche, R. Vanhoutte, S.H.L. Verhelst, Curr. Top. Microbiol. Immunol. 420 (2019) 253–281.
[48] C. Tribet, R. Audebert, J.L. Popot, Proc. Natl. Acad. Sci. U. S. A. 93 (1996) 15047–15050.
[49] J.L. Popot, Annu. Rev. Biochem. 79 (2010) 737–775.
[50] M. Zoonens, F. Giusti, F. Zito, J.L. Popot, Biochemistry 46 (2007) 10392–10404.
[51] M. Zoonens, J.L. Popot, J. Membr. Biol. 247 (2014) 759–796.
[52] X.C. Bai, C. Yan, G. Yang, P. Lu, D. Ma, L. Sun, R. Zhou, S.H. Scheres, Y. Shi, Nature 525 (2015) 212–217.
[53] I.G. Denisov, S.G. Sligar, Chem. Rev. 117 (2017) 4669–4713.
[54] J.F. Bada Juarez, A.J. Harper, P.J. Judge, S.R. Tonge, A. Watts, Chem. Phys. Lipids 221 (2019) 167–175.
[55] Z. Stroud, S.C.L. Hall, T.R. Dafforn, Methods 147 (2018) 106–117.
[56] T.H. Bayburt, Y.V. Grinkova, S.G. Sligar, Nano Lett. 2 (2002) 853.
[57] N.R. Civjan, T.H. Bayburt, M.A. Schuler, S.G. Sligar, Biotechniques 35 (2003) 556–560 (562-3).
[58] T.J. Knowles, R. Finka, C. Smith, Y.P. Lin, T. Dafforn, M. Overduin, J. Am. Chem. Soc. 131 (2009) 7484–7485.
[59] A.O. Oluwole, B. Danielczak, A. Meister, J.O. Babalola, C. Vargas, S. Keller, Angew. Chem. Int. Ed. Engl. 56 (2017) 1919–1924.
[60] M. Barniol-Xicota, S.H.L. Verhelst, J. Am. Chem. Soc. 140 (2018) 14557–14561.
[61] N. Hellwig, O. Peetz, Z. Ahdash, I. Tascon, P.J. Booth, V. Mikusevic, M. Diskowski, A. Politis, Y. Hellmich, I. Hanelt, E. Reading, N. Morgner, Chem. Commun. (Camb.) 54 (2018) 13702–13705.
[62] N.J. Harris, E. Reading, K. Ataka, L. Grzegorzewski, K. Charalambous, X. Liu, R. Schlesinger, J. Heberle, P.J. Booth, Sci. Rep. 7 (2017) 8021.
[63] S.P. Manandhar, E.R. Hildebrandt, W.K. Schmidt, J. Biomol. Screen. 12 (2007)

983–993.
[64] M.S. Shearman, D. Beher, E.E. Clarke, H.D. Lewis, T. Harrison, P. Hunt, A. Nadin, A.L. Smith, G. Stevenson, J.L. Castro, Biochemistry 39 (2000) 8698–8704.
[65] H.F. Dovey, V. John, J.P. Anderson, L.Z. Chen, P. de Saint Andrieu, L.Y. Fang, S.B. Freedman, B. Folmer, E. Goldbach, E.J. Holsztynska, K.L. Hu, K.L. Johnson-Wood, S.L. Kennedy, D. Kholodenko, J.E. Knops, L.H. Latimer, M. Lee, Z. Liao, I.M. Lieberburg, R.N. Motter, L.C. Mutter, J. Nietz, K.P. Quinn, K.L. Sacchi, P.A. Seubert, G.M. Shopp, E.D. Thorsett, J.S. Tung, J. Wu, S. Yang, C.T. Yin, D.B. Schenk, P.C. May, L.D. Altstiel, M.H. Bender, L.N. Boggs, T.C. Britton, J.C. Clemens, D.L. Czilli, D.K. Dieckman-McGinty, J.J. Droste, K.S. Fuson, B.D. Gitter, P.A. Hyslop, E.M. Johnstone, W.Y. Li, S.P. Little, T.E. Mabry, F.D. Miller, J.E. Audia, J. Neurochem. 76 (2001) 173–181.
[66] R.S. Doody, R. Raman, M. Farlow, T. Iwatsubo, B. Vellas, S. Joffe, K. Kieburtz, F. He, X. Sun, R.G. Thomas, P.S. Aisen, E. Siemers, G. Sethuraman, R. Mohs, N. Engl. J. Med. 369 (2013) 341–350.
[67] O.A. Pierrat, K. Strisovsky, Y. Christova, J. Large, K. Ansell, N. Bouloc, E. Smiljanic, M. Freeman, ACS Chem. Biol. 6 (2011) 325–335.
[68] A.R. Sherratt, D.R. Blais, H. Ghasriani, J.P. Pezacki, N.K. Goto, Biochemistry 51 (2012) 7794–7803.
[69] E.V. Wolf, A. Zeissler, S.H. Verhelst, ACS Chem. Biol. 10 (2015) 2325–2333.
[70] E.V. Wolf, A. Zeissler, O. Vosyka, E. Zeiler, S. Sieber, S.H. Verhelst, PLoS One 8 (2013) e72307.
[71] Y. Wang, Y. Zhang, Y. Ha, Nature 444 (2006) 179–180.
[72] Z. Wu, N. Yan, L. Feng, A. Oberstein, H. Yan, R.P. Baker, L. Gu, P.D. Jeffrey, S. Urban, Y. Shi, Nat. Struct. Mol. Biol. 13 (2006) 1084–1091.
[73] A. Ben-Shem, D. Fass, E. Bibi, Proc. Natl. Acad. Sci. U. S. A. 104 (2007) 462–466.
[74] M.J. Lemieux, S.J. Fischer, M.M. Cherney, K.S. Bateman, M.N. James, Proc. Natl. Acad. Sci. U. S. A. 104 (2007) 750–754.
[75] L. Feng, H. Yan, Z. Wu, N. Yan, Z. Wang, P.D. Jeffrey, Y. Shi, Science 318 (2007) 1608–1612.
[76] J. Hu, Y. Xue, S. Lee, Y. Ha, Nature 475 (2011) 528–531.
[77] X. Li, S. Dang, C. Yan, X. Gong, J. Wang, Y. Shi, Nature 493 (2013) 56–61.
[78] M.S. Wolfe, Biochim. Biophys. Acta 1828 (2013) 2886–2897.
[79] L. Sun, L. Zhao, G. Yang, C. Yan, R. Zhou, X. Zhou, T. Xie, Y. Zhao, S. Wu, X. Li, Y. Shi, Proc. Natl. Acad. Sci. U. S. A. 112 (2015) 6003–6008.
[80] K.R. Vinothkumar, K. Strisovsky, A. Andreeva, Y. Christova, S. Verhelst, M. Freeman, EMBO J. 29 (2010) 3797–3809.
[81] E.V. Wolf, S.H. Verhelst, Biochimie 122 (2016) 38–47.
[82] A. Ticha, S. Stanchev, K.R. Vinothkumar, D.C. Mikles, P. Pachl, J. Began, J. Skerle, K. Svehlova, M.T.N. Nguyen, S.H.L. Verhelst, D.C. Johnson, D.A. Bachovchin, M. Lepsik, P. Majer, K. Strisovsky, Cell Chem. Biol. 24 (2017) 1523–1536 (e4).
[83] S. Cho, R.P. Baker, M. Ji, S. Urban, Nat. Struct. Mol. Biol. 26 (2019) 910–918.
[84] G. Yang, R. Zhou, Q. Zhou, X. Guo, C. Yan, M. Ke, J. Lei, Y. Shi, Nature 565 (2019) 192–197.
[85] R. Zhou, G. Yang, X. Guo, Q. Zhou, J. Lei, Y. Shi, Science 363 (2019).
[86] H. Acx, L. Chavez-Gutierrez, L. Serneels, S. Lismont, M. Benurwar, N. Elad, B. De Strooper, J. Biol. Chem. 289 (2014) 4346–4355.
[87] M. Szaruga, B. Munteanu, S. Lismont, S. Veugelen, K. Horre, M. Mercken, T.C. Saido, N.S. Ryan, T. De Vos, S.N. Savvides, R. Gallardo, J. Schymkowitz, F. Rousseau, N.C. Fox, C. Hopf, B. De Strooper, L. Chavez-Gutierrez, Cell 170 (2017) 443–456 e14.
[88] R.P. Baker, S. Urban, Nature 523 (2015) 101–105.
[89] A.J.B. Kreutzberger, M. Ji, J. Aaron, L. Mihaljevic, S. Urban, Science 363 (2019).
[90] W.L. Delano, (2002).